Design Options to Reduce Specific Energy Consumption in Aluminium Electrolysis Cells

Dagoberto Schubert Severo[1] and Vanderlei Gusberti[2]
1. Director,
2. Engineer
CAETE Engenharia Ltda, Porto Alegre, RS, Brazil
Corresponding author: dagoberto@caetebr.com

Abstract

The aluminium smelting industry is facing a period of economic challenge, where the aluminium price is down due to a supply-demand imbalance. The industry is now seeking ways to reduce costs in order to remain competitive. One of the few options that the aluminium smelters have is to reduce energy consumption, since it represents around 35 % of the production cost. Design options to reduce energy consumption by two ways are presented. One way is reducing the heat generated by Joule effect in the cathode and anode conductors, including an innovative design feature to reduce voltage drop in the anode. Another way is reducing the heat losses through the anode and cathode panel. These concepts can be used in existing technologies. Numerical models were used to predict the behaviour of these options and their impact on the cell thermal balance. Approximately 0.8 kWh/kg Al saving is predicted after implementation of all options presented in this paper.

Keywords: Aluminium electrolysis cells; energy consumption; anode design; cathode lining; thermal balance.

1. Introduction

The history of the aluminium smelter industry has shown a continuous decrease of specific energy consumption (SEC) in the reduction of alumina. It was a long road from the 30 kWh/kg Al consumption in the 1900's to the present world average of 13.5 kWh/kg Al, according to IAI [1]. Nevertheless, the reduction rate has stalled in the last 40 years. Only recently some initiatives towards less than 12.0 kWh/kg Al have been published by RTA [2] and Hydro [3].

However, as Barry Welch has pointed out [4] there are many constraints in the present technology, if one is seeking even lower values towards the theoretical minimum of approximately 6.3 kWh/kg Al. The main constraints are related to:

- The unavoidable energy wasted in the busbar used to link one cell to the next;
- The energy associated with the bath superheat required for alumina dissolution and for keeping a stable ledge protection, since there is no sidewall material that resists the liquid bath exposure;
- The preheating of gross carbon, cover, impurities and alumina;
- The inevitable heat losses associated with keeping the cell operating at high temperature.

Some of the typical strategies used to reduce SEC are: decreasing bath heat generation by lowering anode-to-cathode distance (ACD) [5], which requires a very stable pot regarding MHD; reducing the current density by increasing anode and cathode area while keeping the cell current constant; reducing anode bubbles voltage drop which may be achieved by using slots [6] and some latest ideas such as anodes with holes [7] to extract the gases. These strategies are not the focus of this paper, which will be on design options for anodes and cathodes seeking to reduce voltage drop and heat losses.

1.1 Reducing heat losses

The purpose of the anode cover, which usually consists of a mix of crushed bath and alumina, is to thermally insulate the top of the anode block, while preventing its oxidation. Its composition and thickness controls the heat losses through the cover but there are limits for both. Increasing alumina content reduces thermal conductivity but crust stability may be put at risk. In addition, there is a physical limitation to increase thickness related to the yoke position that cannot be covered to avoid its oxidation. The thermal conductivity of the anode cover material changes during anode life due to penetration of bath vapours that consolidates the bottom part of the loose layer in a hard portion [8]. This part has a much higher thermal conductivity and starts to become hard at around 725 ºC [9]. For this reason, the reduction of the thermal losses at the anode by increasing the thickness of the anode cover is limited.

Insulating the sidewall is not new in cell design [10], but should be employed carefully to avoid cell operation without enough ledge protection. There is a limit in heat losses reduction, which is related to limitations in space and the type of materials that can be used in cell construction.

1.2 Reducing voltage drop

Reducing voltage drop in anodes is found in papers [11] and patents such as: US7192508 B2, US5538607 and US6977031 B1. Some ideas of how to improve the contact between cast iron and carbon were studied. They are either related to stub hole design [12] or the one proposed by Berends [13] that uses multiple steel conductors driven into carbon and bonded into the cast iron.

There are many options regarding the reduction of voltage drop in cathodes. Increasing cathode block length decreases cathode voltage drop. Extra care should be taken with side lining insulation due to the reduction of the distance between sides of cathode block and the shell. Increasing collector bar section reduces voltage drop but the side effect is that it increases heat dissipation. Also, there is a limit related to increasing risk of cracks due to block strength reduction in the region around the bar. The use of graphitic and graphitized cathode carbon blocks also reduces voltage drop.

More recently, Feng [14] showed the results of the so called novel structure cathodes (NSC), which are being used in China with success in cells operating at around 12 kWh/kg Al of SEC.

An interesting option to reduce cathode voltage drop is the use of copper inserts in the steel collector bar. It has been tested by the industry since the 1970's (patent US3551319) with a strong renewed interest around end of 1990's (patents US 5976333, US 6231745 B1 and WO2001063014 A1). However, at the same time that copper collector bars reduce the voltage drop, they affect the cell thermal balance by extracting more heat due to the high thermal conductivity of copper. Therefore, it is very useful in a project employing higher current, but it should be used carefully in a project targeting lower energy consumption.

The main problem in reducing the electrical resistance of the conductors, such as anode or cathode, is that this always results in a decrease in the thermal resistance of the assembly. The electrode extracts more heat from the bath and, coupled with the fact that less Joule heat is generated, more heat generation by ACD is therefore required to keep the thermal balance of the cell. As a result, at the same cell current, the SEC increases or stays at the same value.

2. Model Description

A fully coupled thermo-electro-mechanical 3D model in ANSYS was used to predict the behavior of the anode design options. The model is a half anode assembly submodel as shown in Figure 1b. A quarter cell coupled thermo-electro model in Autodesk Simulation (Figure1a) was used to predict the results of the cathode design options. This model was also used to evaluate the impact on the thermal balance of the cell. The material properties used are found in the literature [15, 16]. The cell modeled is a 250 kA side-riser cell designed by CAETE.

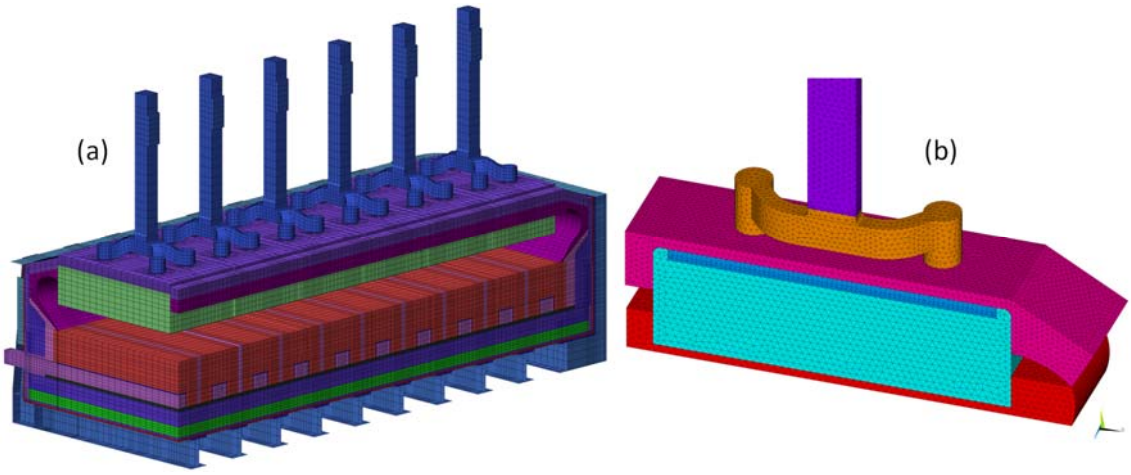

Figure 1. FEA Models – quarter cell (a) and half anode (b).

3. Anode Design Options

The low SEC anode proposed in this work is shown in Figure 2. It consists of an aluminium rod (7), yoke and stubs of steel (6) rodding in the carbon block (1) with cast iron (3). The stub has an internal thermal insulation of ceramic blanket (4) and there is an aluminium insert (2) inside the carbon just below the stub. The top of the carbon block contains a calcium silicate (CaSi) insulation board (5).

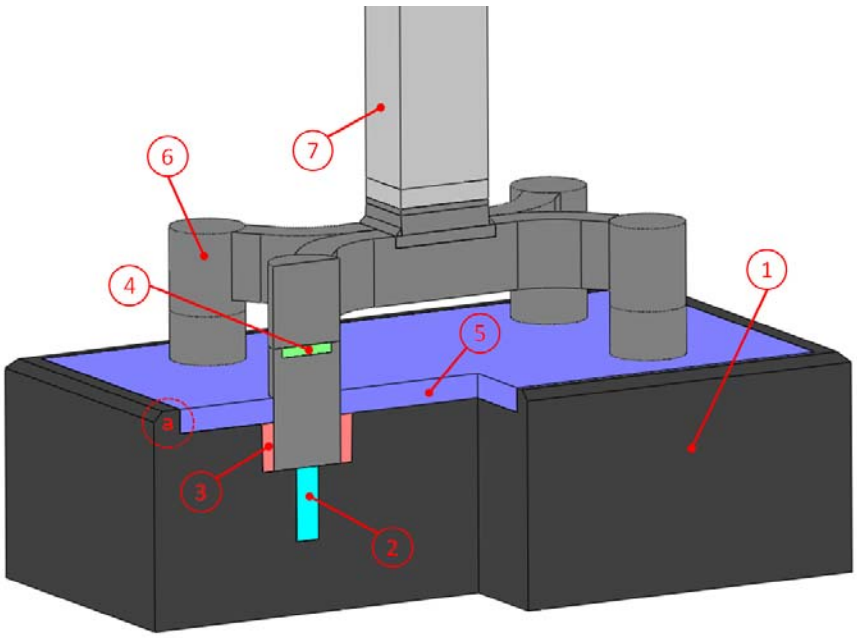

Figure 2. Proposed low SEC anode design.

It is well known that the electrical current flows through the side of the stub to the carbon it is in contact with, and that no current flows through the bottom of the stub [15] because there is no contact pressure. The contact pressure at the sides of the stub is due to the higher thermal expansion of the steel relative to the carbon.

Our innovative idea to reduce the total anode voltage drop is to use an insert (2) made of aluminium located just below the stub. The insert will become liquid at operating temperature which will assure the contact between the carbon and the bottom of the stub. When the anode carbon consumption reaches the bottom of the insert, the aluminium will be released to the metal pool. The hole that remains should be filled with gases released by the alumina reduction reaction and no direct contact of stub with bath should occur. Figure 3 shows the comparison between conventional and low SEC anodes for the voltage drop. Figure 4 shows the comparison for the electrical current density, where we can note the current flowing through the bottom of the stub.

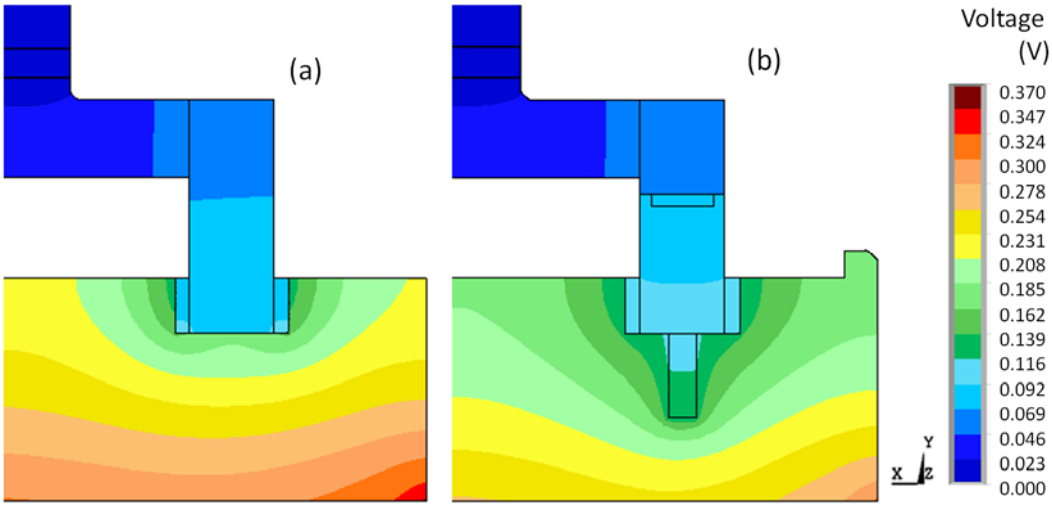

Figure 3. Voltage drop map – conventional anode (a) and low SEC anode (b).

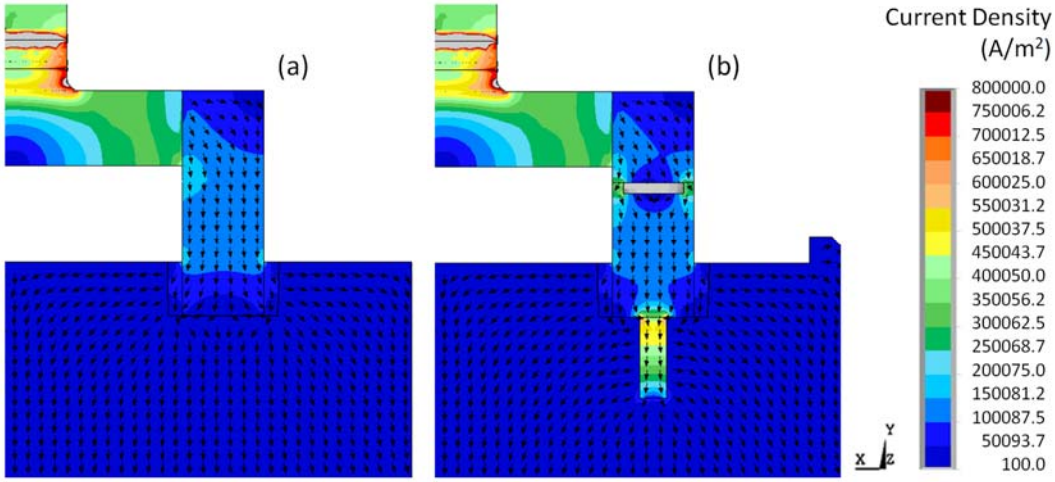

Figure 4. Electrical current density - conventional anode (a) and low SEC anode (b).

One important question is – will the liquid aluminium diffuse into the carbon anode during the around 23 days of anode life? To answer this question we performed a diffusion experiment that consisted of a 20 mm length and 10 mm diameter cylinder of aluminium inside a 50 mm diameter of anode carbon, sealed inside a steel casing to avoid carbon oxidation. The sample

was kept inside a furnace at 850 ºC for 23 days, without electrical current. The Figure 5 shows the section of the diffusion test cell after this period where there are no signs of aluminium inside the carbon. X-Ray diffraction analysis was done in the material found at the carbon/aluminium interface of the sample and it is shown in Figure 6. We can notice that in the interface of aluminium with the carbon, Al_4C_3 was found, which may explain why the aluminium did not diffuse through the carbon.

(a) (b)

Figure 5. Diffusion test cell (a) and the aluminium test cylinder (b).

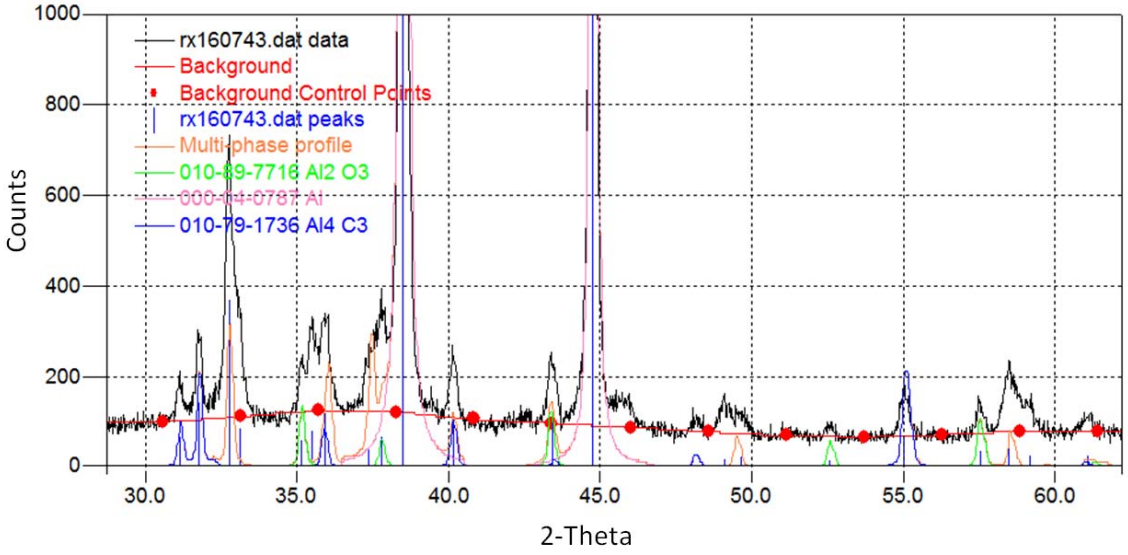

Figure 6. X-Ray diffraction analysis graph.

The longer the insert is, the higher is the voltage reduction, but with lower effective time before the anode consumption reaches its bottom. Therefore, an optimization study was run over time and the average anode panel total electrical resistance was calculated. The results showed that the optimum length is around 150 mm length for a 50 mm insert diameter. The Figure 7 shows the heat flux for the conventional and the low SEC anodes.

Our proposal to reduce heat losses through the stubs is to create a thermal barrier in the middle of it. This thermal barrier creates a higher localized voltage drop and should be well designed to

avoid an overall negative impact on the energy consumption. The barrier may be installed when replacing the stub during routine maintenance of the anode assemblies.

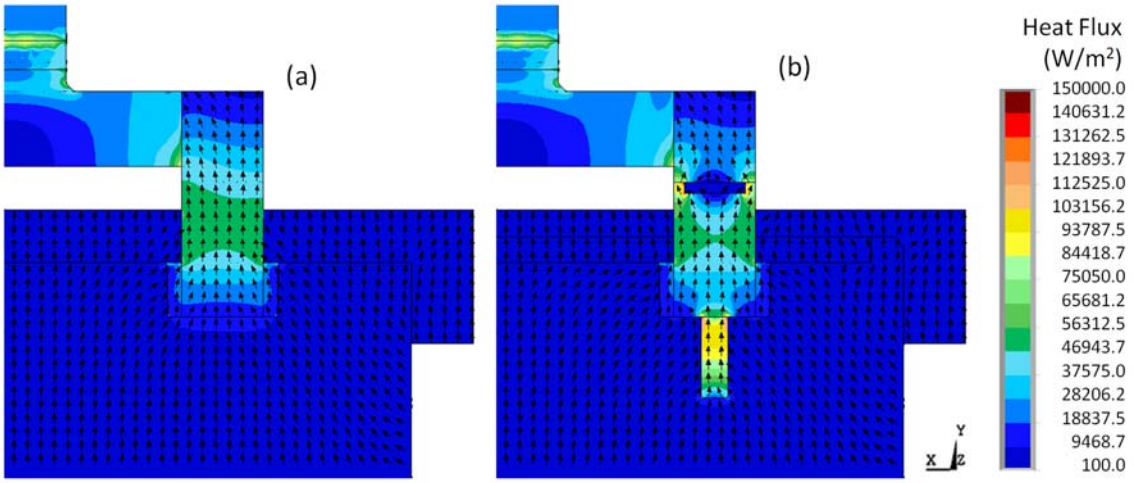

Figure 7. Heat flux – conventional anode (a) and low SEC anode (b).

In order to reduce the anode top heat losses, we are proposing a solid cover of calcium silicate board of 50 mm thickness and conventional mix cover of 50 % crushed bath and 50 % alumina on top of it. To protect the calcium silicate from bath attack, the board is installed in a recess in the anode – see detail "a" in Figure 2. Figure 8a shows the isotherms for the conventional anode and Figure 8b shows them for the low SEC anode. We can notice that the top of the calcium silicate board presents around 500 ºC and the cover on its top shall not become hard. Therefore, it is not losing its thermal insulation value. Due to the high cost of calcium silicate boards, it is necessary to design a method to recover it. Otherwise, long term contamination of the anode cover material recycle with Ca and Si need to be addressed in the butt cleaning process. A low cost option is ceramic fiber blanket which has the advantage of dealing only with Si contamination.

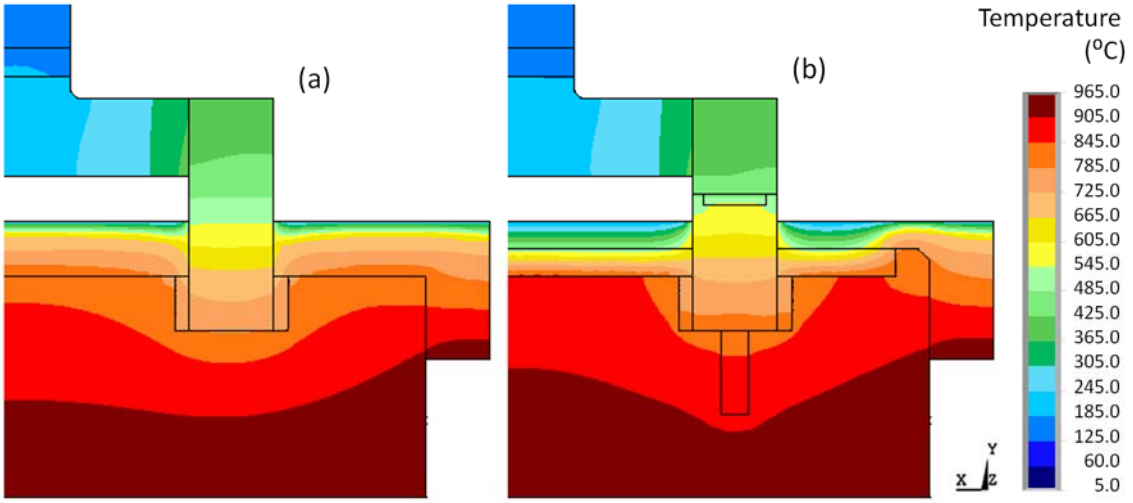

Figure 8. Temperature map – conventional anode (a) and low SEC anode (b).

In order to study and to understand the thermal behavior of the anode assembly, it is possible to choose a control volume that involves only the anode, its cover, yoke and rod as presented in Figure 9.

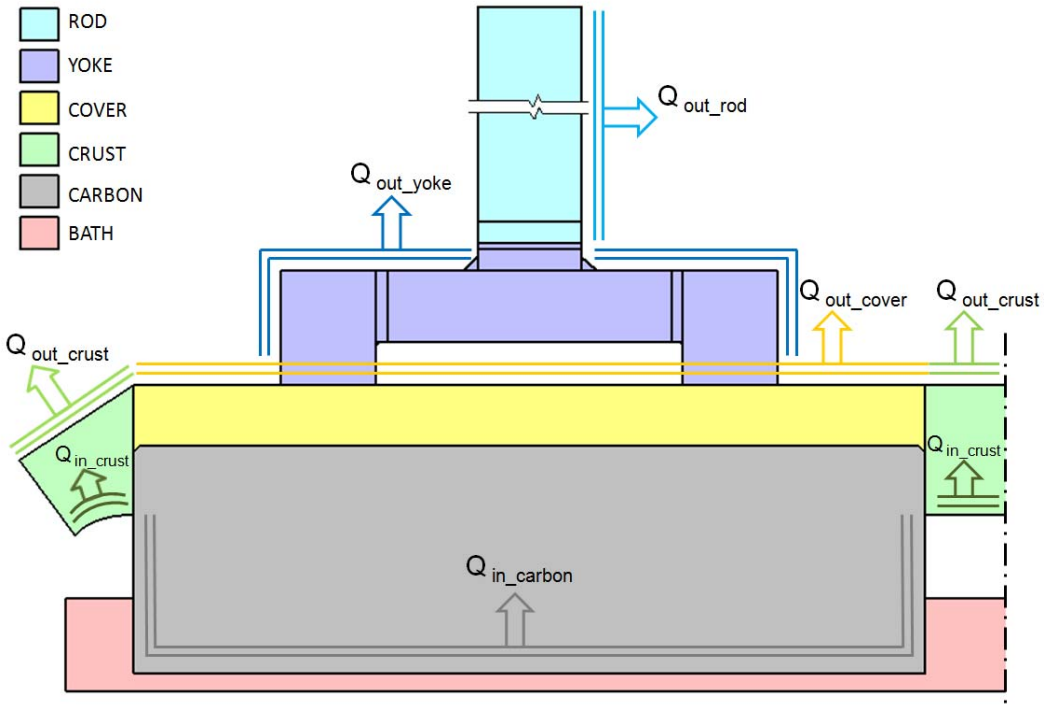

Figure 9. Heat balance for an anode assembly control volume.

The heat balance in steady state for this control volume can be written as:

$$Q_{in\_carbon} + Q_{in\_crust} + q_{gen} = Q_{out\_crust} + Q_{out\_cover} + Q_{out\_yoke} + Q_{out\_rod} \quad (1)$$

where:

Q_{in_carbon}	Heat entering the anode carbon bottom surface, W
Q_{in_crust}	Heat entering the crust facing the bath, W
q_{gen}	Heat generated by Joule effect in the electrical conductors, W
Q_{out_crust}	Heat leaving the crust surface, W
Q_{out_cover}	Heat leaving the anode cover surface, W
Q_{out_yoke}	Heat leaving the yoke and stubs surfaces, W
Q_{out_rod}	Heat leaving the rod surface, W

Table 1 presents the model results for the studied cases. The base case is A1 where a conventional anode was run in the model. In case A2 only the aluminium insert is applied in the anode, in case A3 only the CaSi top board is applied, and in case A4 only the insulated stub is used. Case A5 is the combination of A3 and A4. Case A6 is the combination of A2, A3 and A4.

We can note that the gain of 57 mV in the anode voltage drop that results from the use of the aluminium insert (case A2) is almost all compensated by the extra heat input in the carbon, which explains why there is only 17.9 kWh/t Al of SEC gain. Insulating the stub (case A4) increases the anode IR SEC but decreases the heat input, resulting in a net SEC gain of 43 kWh/t Al. The big individual gain is the case A3, which reduces the heat dissipation through the top of the anode resulting in a SEC gain of 248.5 kWh/t Al. The combination of all the features (case A6) results in a SEC gain of 314.7 kWh/t Al.

Table 1. Summary of model results for the low SEC anode cases.

Case		A1	A2	A3	A4	A5	A6
Cell current	(kA)	250.0	250.0	250.0	250.0	250.0	250.0
Anode IR	(V)	0.321	0.264	0.321	0.328	0.328	0.271
Heat input							
Q_{in_carbon}	(kW)	100.9	113.7	81.1	95.9	75.24	88.30
Q_{in_crust}	(kW)	24.7	25.4	23.0	24.4	22.57	23.25
q_{gen}	(kW)	80.3	66.0	80.3	81.9	81.88	67.71
Heat losses							
Q_{out_crust}	(kW)	24.7	24.5	25.4	24.8	25.5	25.3
Q_{out_cover}	(kW)	76.7	75.3	53.9	79.0	55.4	54.6
Q_{out_yoke}	(kW)	95.6	96.5	96.2	89.6	90.2	90.9
Q_{out_rod}	(kW)	20.5	20.6	20.6	20.0	20.1	20.1
SEC (95.5 % CE)							
Anode IR	(kWh/t)	1002.4	824.4	1001.7	1022.5	1022.0	845.1
$Q_{in\_carbon} + Q_{in\_crust}$	(kWh/t)	1594.3	1754.5	1346.5	1531.2	1274.0	1436.9
Anode total	(kWh/t)	2596.7	2578.9	2348.2	2553.7	2296.0	2282.0
Difference to A1	(kWh/t)	0.0	-17.9	-248.5	-43.0	-300.8	-314.7

4. Cathode Design Options

The lining for the base case is shown in the Figure 10a. It consists of a SiC sidewall (1), an anthracitic carbon insert (2), ramming paste (3), graphitized grade cathode block (4), high density (HD) vermiculite (5), low density (LD) vermiculite (6), refractory bricks (7), perlite bricks (8) and a steel collector bar (9). The low SEC modification (Figure 10b) uses a copper collector bar (2), removing the carbon insert and using only ramming paste (3), with microporous insulation (6) below the HD vermiculite (5).

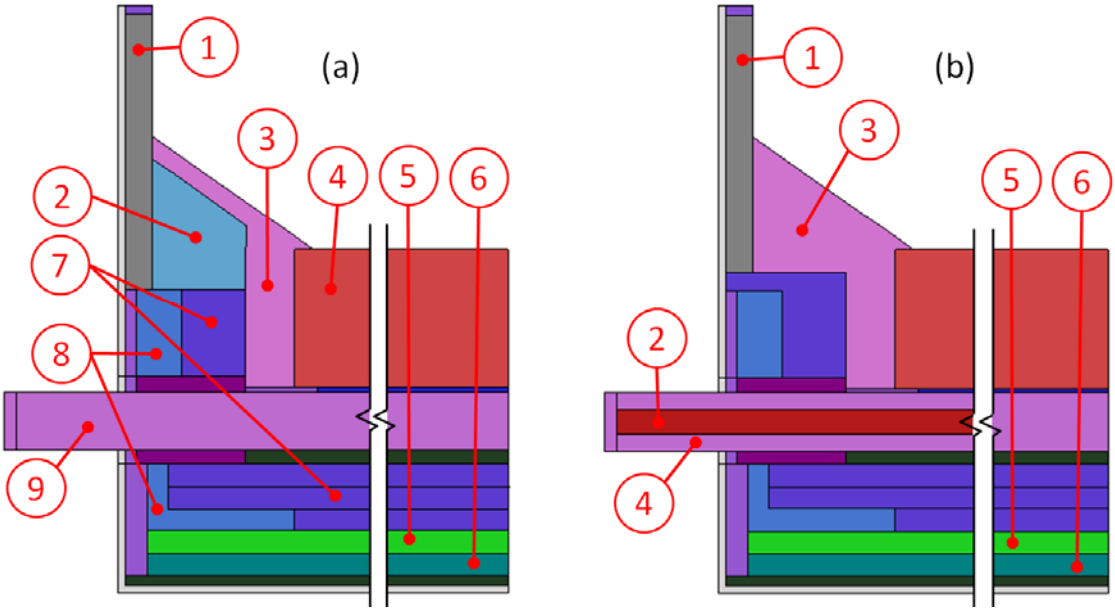

Figure 10. Conventional (a) and a low SEC cathode design (b).

In this work, we propose using copper inserts in the collector bar to reduce cathode voltage drop. Traditional cathode designs with steel bars have from 2 to 0.9 μΩ of total panel resistance that could be reduced by up to 40 % by using copper insert bars according to our experience.

There are limitations regarding the materials that can be used inside the shell casing to reduce cathode heat losses. Insulation material requirements are related also to the compressive crushing strength since one should be able to walk over the insulation material when installing it. Typical materials used as insulation are perlite bricks, vermiculite and calcium silicate boards. Figure 11 shows the thermal conductivity function of temperature for the insulation materials. An option with very low thermal conductivity is microporous insulation [17] which is a material made of pyrogenic silica plus opacifier that presents only 0.04 W/mK at 800 ºC. Microporous insulation is made of 90 % of void volume. The voids are so small that the air trapped is unable to interact with its neighbors in what is known as microporous effect. The cold crushing strength is around 1.0 MPa which is quite similar to low density vermiculite.

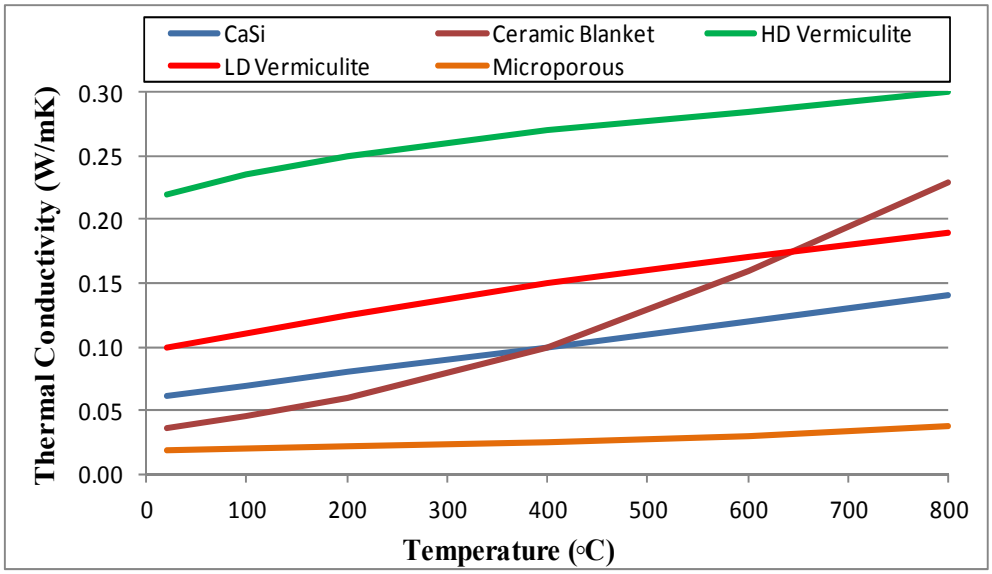

Figure 11. Thermal conductivity of insulation materials.

However, there is a limit to the reduction in heat losses through the bottom of the cell, which is related to the type of sodium barrier used. The most used barrier nowadays is the one that relies on the refractory composition (around 70 % of SiO2) and the generation of the so called "penetration barrier". This barrier occurs at around 850 °C and this isotherm should be inside the refractory bricks, otherwise the thermal insulation would be damaged. This requirement limits the minimum heat loss possible, since typically there is from 250 mm to 350 mm of space below the cathode inside the shell casing. Refractory and insulation materials have to be fitted in this confined space. Figure 12 shows the minimum possible bottom heat losses for the range of sub-cathodic space and for typical materials used as bottom insulation. In this case 830 °C was used as maximum temperature for the hot face of the insulation material.

If the insulation is hotter than the barrier limit, the material will be contaminated. Then it starts to lose its thermal resistance resulting in an increased heat loss over time. A thermal over-insulated bottom lining shows a continuous degradation during the cell life. A possible way to reduce the bottom heat losses is by increasing its thermal resistance using a different barrier such as steel plates [16]. The problem when using low carbon steel is its tendency to oxidize [18] and to lose its efficiency. An option could be the use of stainless steel as a barrier.

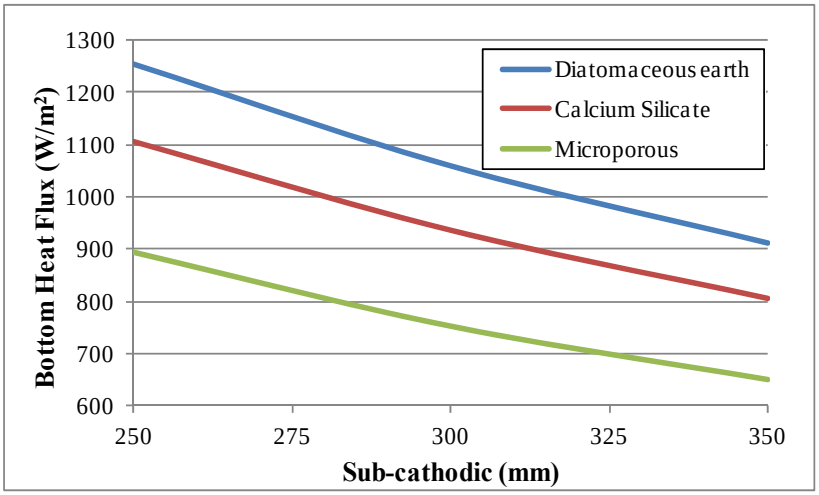

Figure 12. Minimum possible bottom heat flux.

The Figure 13 shows the isotherms comparison between the conventional and the low SEC cathode.

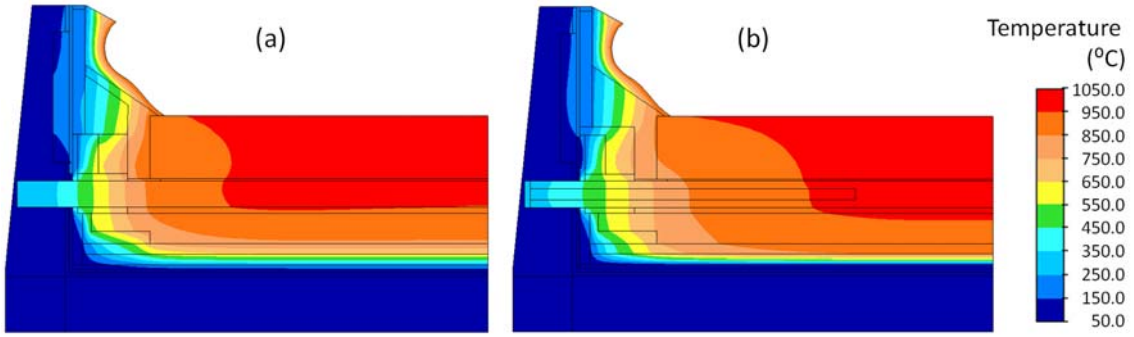

Figure 13. Temperature map – conventional (a) and low SEC cathode (b).

We propose replacing the anthracitic part of the comb-block by ramming paste and to increase the refractory pier at the side of the cathode block in order to improve the sidewall thermal efficiency. In this way, less heat is lost from the side of the cathode block to the SiC sidewall as it is shown in the Figure 14.

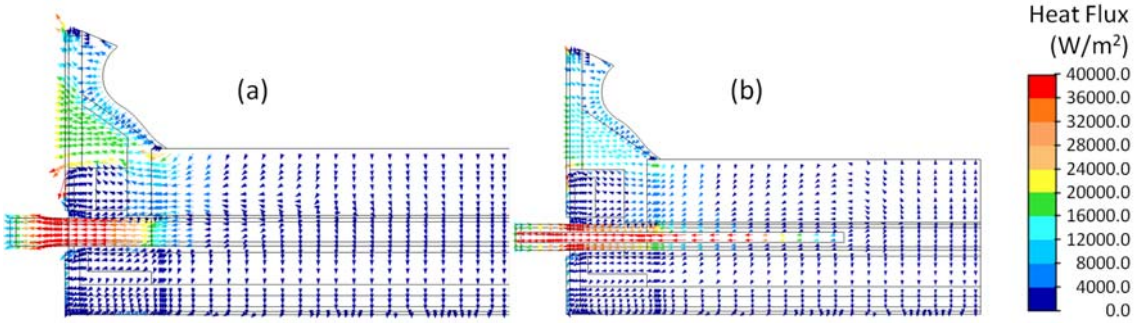

Figure 14. Heat flux vectors – conventional (a) and low SEC cathode (b).

We are also proposing to change the cathode grade from graphitized to graphitic. The use of graphitized cathodes is not the best option in terms of SEC because, when comparing with graphitic blocks, for a gain of 1.6 times in electrical conductivity there is a 2.5 times higher thermal conductivity, which increases the heat flux from the cell cavity to the exterior, despite

the decrease in cathode voltage drop. Table 2 shows the comparison of electrical and thermal properties for the most common cathodes grades.

Table 2. Typical electrical resistivity and thermal conductivity of different cathode grades.

Grade		30 % graphite		graphitic		graphitized	
Direction		M	P	M	P	M	P
Electrical resistivity at 1 000 °C	(μΩm)	22	30	16	20	10	12
Thermal conductivity at 1 000 °C	(W/mK)	13	12	22	18	55	45

M - parallel to extrusion direction (with grain);
P - perpendicular to extrusion direction (against grain).

A control volume can be defined to the cathode panel as presented in Figure 15.

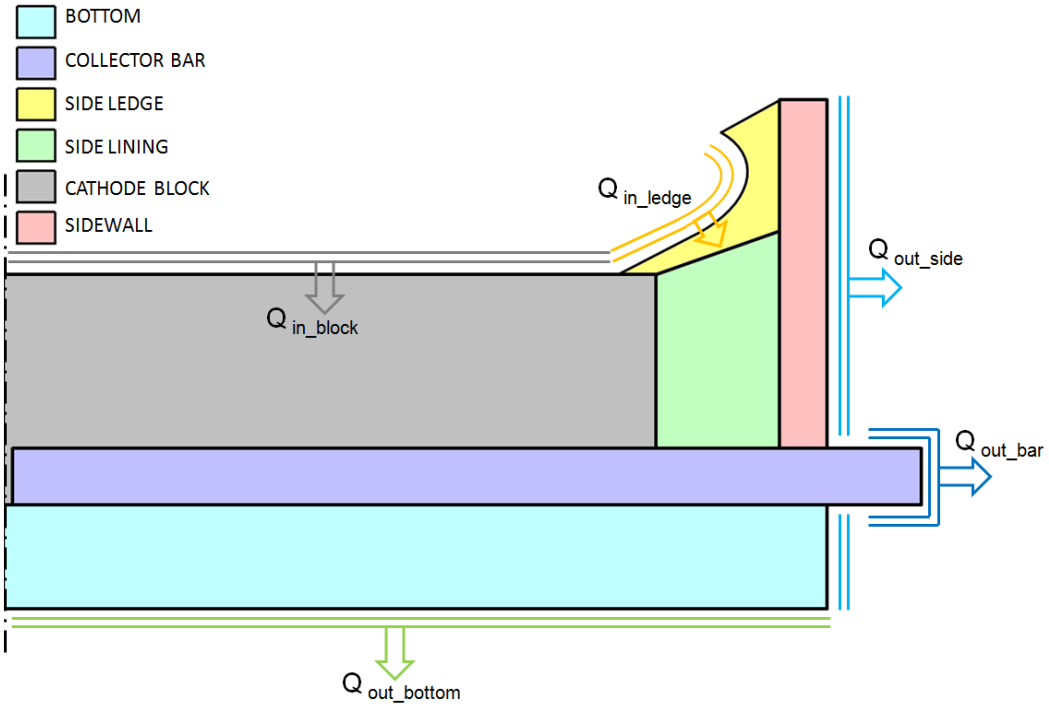

Figure 15. Heat balance for a cathode assembly control volume.

The heat balance in steady state for this control volume can be written as:

$$Q_{in\_block} + Q_{in\_ledge} + q_{gen} = Q_{out\_side} + Q_{out\_bar} + Q_{out\_bottom} \quad (2)$$

where: Q_{in_block} Heat entering the cathode block top surface, W
Q_{in_ledge} Heat entering the side ledge facing the bath and metal, W
q_{gen} Heat generated by Joule effect in the electrical conductors, W
Q_{out_side} Heat leaving the side shell surface, W
Q_{out_bar} Heat leaving the collector bar outside of shell, W
Q_{out_bottom} Heat leaving the bottom of the shell surface, W

Table 3 presents the thermal balance model results for the cathode cases studied. The base case is C1 which is a conventional design. Case C2 is a copper collector bar cathode, case C3 is the insulated bottom, case C4 is an insulated sidewall and case C5 is a graphitic grade cathode block. C6 is the combination of C3, C4 and C5 with anode A5. C7 is the combination of C2, C3, C4 and C5 with anode A6.

Table 3. Summary of model results for the low SEC cathode cases.

Case		C1	C2	C3	C4	C5	C6	C7
Anode		A1	A1	A1	A1	A1	A5	A6
Cell current	(kA)	250.0	250.0	250.0	250.0	250.0	227.0	241.0
Cathode IR	(V)	0.405	0.259	0.405	0.405	0.430	0.390	0.273
Cell voltage	(V)	4.332	4.374	4.240	4.237	4.300	4.080	4.067
ACD	(mm)	43.8	49.7	40.9	40.8	42.0	43.8	43.8
Heat input								
Q_{in_block}	(kW)	85.4	129.6	61.0	61.9	64.0	24.8	65.5
Q_{in_ledge}	(kW)	120.6	123.9	119.9	118.1	127.3	116.5	120.5
q_{gen}	(kW)	101.1	64.9	101.1	101.1	107.4	107.4	70.7
Heat losses								
Q_{out_side}	(kW)	208.3	206.4	208.0	182.2	202.5	176.4	173.9
Q_{out_bar}	(kW)	55.9	70.0	56.5	56.6	54.3	56.0	67.4
Q_{out_bottom}	(kW)	44.1	43.1	18.5	44.1	43.2	18.2	17.4
SEC (95.5 % CE)								
Cathode IR	(kWh/t)	1263.8	808.2	1263.8	1263.8	1341.8	1217.0	851.9
$Q_{in\_block} + Q_{in\_ledge}$	(kWh/t)	2571.7	3163.2	2257.0	2247.2	2388.0	2142.8	2460.2
Cathode total	(kWh/t)	3835.5	3971.4	3520.8	3511.0	3729.8	3359.8	3312.1
Cell total	(kWh/t)	13517.7	13648.7	13230.6	13221.2	13417.8	12731.3	12690.7
Difference to C1	(kWh/t)	0.0	131.1	-287.1	-296.4	-99.9	-786.3	-826.9

The case C2 shows a net increase in SEC, although a gain of 146 mV in the cathode voltage drop is observed, resulting from the use of the copper collector bar. This occurs because the copper insert works as a heat extractor: the extra heat input of 44.2 kW in the block is greater than the gain of 36.2 kW in heat generation. Insulating the bottom (case C3) reduces the heat dissipation and the SEC gain is 287.1 kWh/t Al. The insulated sidewall (case C4) shows a big reduction in heat input at the block resulting in a SEC gain of 296.4 kWh/t Al. The case C6 is a combination of only the options that reduced heat losses, including the A5 anode. This combination was run at lower current using the same ACD of C1 and it results in a SEC gain of 786.3 kWh/t Al. The combination of all the features (case C7) results in a SEC gain of 826.9 kWh/t Al and it was also run at lower current to have the same ACD of C1. We can note that the current decrease was smaller in case C7 than in case C6 while the SEC gain is greater.

6. Conclusions

The relevance of energy efficiency today is increasing, not only due to the rise in energy cost, but mainly due to the intensification of global pressures to reduce greenhouse gas emissions.

In this paper, the design strategy for both anode and cathode design modifications was to reduce as much as possible the conductor electrical resistance while increasing its thermal resistance, thus limiting heat losses. If only the heat losses are reduced, the cell should run at lower current to maintain its thermal balance and this would impact on the cell productivity, and ultimately, on the production cost.

An innovative idea to reduce the anode panel SEC was presented. It consists of an aluminium insert under the stub inside the carbon block, together with a ceramic blanket inside the stub and a calcium silicate insulation board on the top of the carbon block. The new design does not

require modifying anode dimensions, preventing modifications in the rodding shop and baking furnace. The concepts can be used in existing technologies allowing the increase of energy efficiency at a low cost of implementation.

The low SEC anode together with the suggested cathode design results in a SEC gain of more than 800 kWh/t of aluminium with a minor impact on cell productivity.

7. References

1. International Aluminium Institute (IAI), Primary aluminium smelting energy intensity, Date of issue 20 July 2015.
2. O. Martin et al., Low energy cell development on AP technology, *Light Metals* 2012, 569-574.
3. Martin Segatz et al., Hydro's cell technology path towards specific energy consumption below 12 kWh/kg, *Light Metals* 2016, 301-305.
4. Barry Welch, Constraints and options for reducing energy consumption in aluminium smelting, *Proceedings of 31st International ICSOBA Conference*, Krasnoyarsk, Russia, September 4-6 2013.
5. P. Coursel et al., The Transition Strategy at Alouette Towards higher Productivity with a Lower Energy Consumption, *Light Metals* 2012, 591-594.
6. Xiangwen Wang et al., Development and deployment of slotted anode technology at Alcoa, *Light Metals* 2012, 299-304.
7. Feng Naixiang et al., Towards decreasing energy consumption of aluminum reduction by using anodes with holes and channels, *Light Metals* 2014, 517-520.
8. Amal Aljasmi et al., Evaluation of anode cover heat loss, *Proceedings of 33rd International ICSOBA Conference*, Dubai, UAE, 29 November – 1 December 2015, Paper AL10, *Travaux No. 44,* 579-587.
9. K.A. Rye, J. Thonstad, X. Liu, Heat transfer, thermal conductivity, and emissivity of Hall-Héroult top crust, *Light Metals*, 1995, 441-449.
10. Zhou Jianfei and Marc Dupuis, In-depth analysis of lining designs for several 420 kA electrolytic cells, *Light Metals 2012*, 591-594.
11. Dag Sverre Sæsbøe, Storvik high conductivity anode yoke with copper core, *Proceedings of 33rd International ICSOBA Conference*, , Dubai, UAE, 29 November – 1 December 2015, Paper AL23, *Travaux No. 44, 717-726.*
12. Daniel Richard et al., Challenges in stub hole optimisation of cast iron rodded anodes, *Light Metals* 2009, 1067-1072.
13. W. Berends et al., Low resistance anode assembly using steel stubhole conductors across the cast iron to carbon interface, *Light Metals* 2016, 965-969.
14. F. Naixiang et al., Energy reduction technology for aluminum electrolysis: choice of the cell voltage, *Light Metals* 2013, 549-552.
15. Siegfried Wilkening and Jules Côté, Problems of the stub – anode connection, *Light Metals* 2007, 865-873.
16. M. Sorlie, H. Oye, *Cathodes in Aluminium Electrolysis*, 3rd Edition 2010 .
17. Iain Mackenzie, Using microtherm microporous insulation in smelter applications, *JOM February 2000*, Volume 52, Issue 2, 73-73.
18. C. Allaire, Efficiency of steel plate barriers in aluminum reduction cell potlining refractories, *Journal of Canadian Ceramic Society*, May 1994, 128-131.